

Hot-hole lasers in III-V semiconductors.

P. Kinsler* and W.Th. Wenckebach†

Department of Applied Physics, Technical University Delft, Lorentzweg 1, 2628 CJ DELFT, The Netherlands.

Following the success of p-Ge hot-hole lasers, there is also potential for using other semiconductor materials, notably III-V's such as GaAs and InSb. Previous analysis had suggested that a large effective mass ratio between the heavy and light holes is advantageous, which implies that InSb would make an excellent hot-hole laser. Using our Monte Carlo simulations of both GaAs and InSb hot-hole lasers in combination with a rate equation model, we see that previously accepted criteria used to predict performance are not always reliable, and we suggest suitable alternatives. The simulation results include gain and gain bandwidth as a function of field strength and laser frequency, and alternative field orientations and photon polarizations are considered. Comparisons are made with bulk p-Ge systems. The optimum conditions predicted by our simulations could then be used in the design of quantum-well hot-hole lasers.

This paper was published as *J. Appl. Phys.* **90**, 1692 (2001).

I. INTRODUCTION

Hot-hole lasers emit in the THz (far-infrared) with an unusually broad gain spectrum, allowing amplification and generation of laser pulses on a picosecond time scale [1, 2, 3, 4, 5, 6, 7, 8]. This type of laser has been realised in bulk p-doped Germanium (p-Ge), and produced gains of about 0.25cm^{-1} . Since the THz band has important potential applications in medical imaging and short-range (e.g. office) communications, and due to the widespread applications of GaAs [9, 10, 11], there has been interest in the potential of III-V materials such as GaAs and InSb as hot-hole lasers. Most predictions have been based on simple scattering rate and effective mass arguments (see e.g. [1]); so to investigate the possibilities of III-V materials more thoroughly we have done a set of Monte Carlo simulations for both GaAs and InSb. We cover a range of field strengths, orientations, and doping concentrations.

Hot-hole lasers usually consist of a p-doped Ge crystal in a cryostat cooled to about 20K, with crossed electric and magnetic fields applied, and are described extensively in Ref. [1]. In this system, the ideal lasing cycle for a hole is depicted in Fig. 1 as follows: (1) the electric field accelerates a heavy hole to above the optical phonon energy ϵ_{LO} , (2) the hole scatters into the light hole band by emitting an optical phonon, (3) due to its lighter mass, the hole is now localised on a closed cyclotron orbit in the light hole band, and this localisation forms an inversion, and so (4) stimulated emission of a photon transfers the hole from the light back to the heavy hole band. In order to get the streaming motion (1) combined with the cyclotron orbits of (3) it is necessary to apply the correct ratio of electric to magnetic field strengths as determined by the heavy to light hole effective mass ratio. If this is not done we

may get cyclotron orbits which do not reach ϵ_{LO} in the heavy hole band, or light holes which reach ϵ_{LO} and scatter instead of being localised in cyclotron orbits.

The results we present in this paper are obtained using a Monte Carlo simulation (see section II) which can deal with for bandstructure and scattering processes properly. However, in order to describe the basic mechanism we now present a simple rate equation model.

The holes are, roughly speaking, in one of three different locations: “H” the lower part of the heavy hole band; “H+” the upper part of the heavy hole band (above ϵ_{LO}); and “L” on cyclotron orbits in the light hole band. Holes in “H” stream up to “H+” with rate r_{stream} [12], or their streaming is disrupted by intraband scattering with rate r_{HH} . Holes in “H+” will most likely emit an optical phonon, and either scatter into “L” with rate γr_{OP} , or back into “H” with rate $(1 - \gamma)r_{OP}$. Holes in “L” can either scatter by phonon or impurity processes back into “H”, or emit a photon and scatter into “H” also. This is diagrammatically represented on fig. 1(b), and the populations (N_H, N_{H+}, N_L) in these locations can be described by rate equations:

$$\frac{d}{dt}N_H = -r_{stream}N_H + [(1 - \gamma)r_{OP} + r_{HH}]N_{H+} + r_{LH}N_L \quad (1)$$

$$\frac{d}{dt}N_{H+} = +r_{stream}N_H - [r_{OP} + r_{HH}]N_{H+}, \quad (2)$$

$$\frac{d}{dt}N_L = +\gamma r_{OP}N_{H+} - r_{LH}N_L, \quad (3)$$

where γ is the fraction of optical phonon emissions which end up in the LH band. Using a density of states ratio argument and $m_{HH} \gg m_{LH}$, this is $\gamma \approx (m_{HH}/m_{LH})^{-3/2}$. Note that this model says nothing about the inversion, which is localised in k space.

None of the steps in the ideal lasing cycle (1-4) are very efficient, and so it is best to regard the hole transport as being predominantly a sea of unhelpful scatterings with the lasing cycle superimposed on top of it. It is only if we can make the lasing cycle strong enough by selecting a suitable material, and adjusting the field strengths, field directions, or doping concentration will we see lasing. Past analysis of the lasing cycle has provided number of criteria that are usually used to determine whether steps (1-4) will be sufficiently strong

*Electronic address: Dr.Paul.Kinsler@physics.org; New address: Department of Physics, Imperial College, Prince Consort Road, London SW7 2BW, United Kingdom.

†Electronic address: wenckebach@tn.tudelft.nl

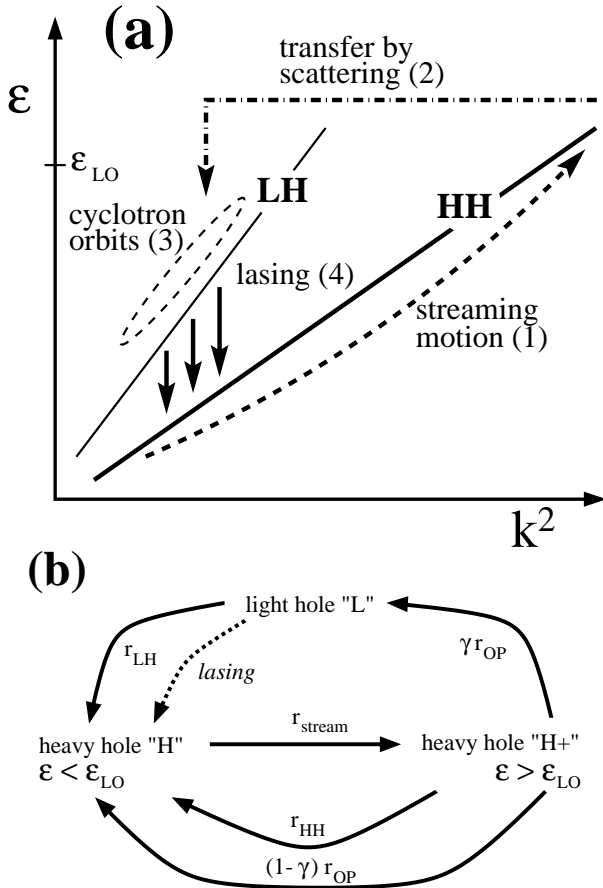


FIG. 1: The hot-hole laser: (a) shows the streaming motion up the heavy hole band (1), the scattering to the light hole band (2), the cyclotron orbits in the light hole band (3), and the lasing transition (4); (b) shows a simple three-state model of the operation of the laser, with the transition rates being: r_{stream} the rate of streaming up HH to above the optical phonon energy, r_{OP} the optical phonon emission rate, r_{HH} the HH intra-band scattering rate, and r_{LH} the rate of depopulation of the LH band.

[13, 14, 15]. In particular, criteria for the temperature and electric and magnetic field strengths were given to ensure that the heavy and light holes would be unlikely to scatter below the optical phonon energy; that heavy holes do scatter when above this energy; and that some of these scattered holes reach the light hole band. They also favoured a high effective mass ratio m_{HH}/m_{LH} , such as that in InSb, making it easier to ensure that the heavy holes are accelerated to the optical phonon energy whilst the light holes remain in closed orbits. We show here that such arguments, especially the latter, do not always hold true.

II. SIMULATIONS

The simulations were done in two stages. First, for chosen electric (E) and magnetic (B) field directions (i.e.

$E[01\bar{1}]B[100]$; $E[112]B[1\bar{1}0]$; $E[2\bar{1}\bar{1}]B[0\bar{1}1]$; $E[\bar{1}\bar{1}1]B[112]$ – see [16]), one Monte Carlo simulation was done for each point of a grid of field strengths covering the range of interest. The simulations produced distribution functions of heavy and light holes and the average scattering times for the system under the chosen conditions. The second stage used the distributions to calculate inversion-gain cross-sections σ_I ; and the average scattering times were used in a Drude model to calculate the optical absorption σ_a . These two were then combined and multiplied by the impurity concentration n_i to give the net gain per unit length $\lambda = (\sigma_I - \sigma_a)n_i$ as a function of photon frequency for each grid point. This three dimensional dataset of net gains was then analyzed to produce contour plots of maximum gain, enabling us to see the best directions and strengths of E and B to choose to get optimum gain.

Our Monte Carlo simulations[17] of this system include a full $k.p$ band structure calculation [18] and all important scattering processes: optical phonon scattering due to deformation potential (OPD) and polar interactions (OPP), acoustic phonon scattering due to deformation potential (ACD) and piezoelectric interactions (ACP), and (Coulomb) ionized impurity (IIM) scattering [19, 20]. We treat the effect of the electric and magnetic fields classically, giving the holes continuous trajectories in k -space – comparison with experiment for p-Ge systems indicates that this approximate treatment is adequate for the field strengths we consider. All simulations are done at a lattice temperature of 20K. They follow the progress of a single hole through a large number of scatterings (typically ~ 16000), with the ergodic theorem being used to justify the use of the simulation's time-average as an ensemble average. Since both the hole-hole scattering processes and ionized impurity scatterings are mediated by screened coulomb potentials, this means that hole-hole scattering can be allowed for by doubling the impurity concentration in the simulation – since the hole concentration is equal to the impurity concentration [21].

The Monte Carlo simulations used the standard overestimation technique where for each scattering process the post-scattering direction of the hole was chosen at random, and the differential scattering rate was overestimated by an isotropic rate just higher than its maximum value. However, this proved to be very slow for the ionised impurity scattering, especially at low impurity concentrations. Therefore, in this case we weighted the choice of scattering angle by the angular dependence of the scattering rate, and thus avoided generating a large proportion of inefficient overestimations.

Optical absorption was estimated using a Drude free carrier model, which uses zone centre effective masses and the hole scattering times calculated in the Monte Carlo simulations. This model assumes that each scattering completely randomises the phase of the particle. However, IIM scattering, which makes a significant contribution to the average hole scattering times, involves a large proportion of scatterings which only slightly deflect the hole. As a result, the ordinary treatment of IIM scattering would significantly overestimate the scattering rate used to calculate the optical absorption. We avoid this problem because our IIM algorithm weights the choice of angle, while the scattering rate itself

is isotropic. By choosing an algorithm compatible with our model of optical absorption, we achieved both an efficient model of IIM scattering whilst avoiding the necessity of a more complex absorption model.

III. GERMANIUM

To validate our model and simulation code, we first did some simulations of hot-hole lasers in p-Ge and compared our results against those typically given in the literature. The optimum gain contour plots are shown on fig. 2, and table I shows the relative frequencies of the different scattering types at the point of optimum gain. The columns ACD, IIM, and OPD on this table refer to the acoustic phonon, ionised impurity, and deformation potential optical phonon scattering processes respectively. These simulations also provided us with a good reference with which our GaAs and InSb simulation results can be compared. The results, for an impurity concentration of $n_i = 0.025 \times 10^{16} \text{cm}^{-3}$, are shown in Fig. 2, where the optimum gain is about $0.25/\text{cm}$ at $F = 5 \text{kV/cm}$ $[2\bar{1}\bar{1}]$ and $B = 4 \text{T}$ $[0\bar{1}1]$.

TABLE I: The relative frequencies of different scattering types in Ge at a point of optimum gain: $E = 5 \text{kV/cm}$ $[2\bar{1}\bar{1}]$, $B = 4 \text{T}$ $[0\bar{1}1]$ and $n_i = 0.025 \times 10^{16}$. There were a total of 16000 scatterings, and the hole was in the LH band for $250 \pm 44 \text{ps}$, and the HH band for $1076 \pm 49 \text{ps}$. The average time between collisions in the LH and HH bands were $t_{LH} = 4.9 \text{ps}$ and $t_{HH} = 1.1 \text{ps}$ respectively. NB: $m_{HH}/m_{LH} \approx 8$; $r_{stream} \approx 1.3 \text{ps}^{-1}$;

Transition	ACD	IIM	OPD	Total
HH \rightarrow HH	749	161	13619	14529
HH \rightarrow LH	48	8	612	676
LH \rightarrow LH	4	95	21	120
LH \rightarrow HH	158	90	428	676

These simulations also enabled us to test the accuracy of our simple model of optical absorption against the more sophisticated model of Lok [16, 22], which included second order transitions of phonons and photons, or ionised impurities and photons; while all scattering processes were taken into account. We obtained optical absorptions within $\sim 25\%$ of Lok at photon energies of 5meV – due to the inverse dependence of absorption with frequency, the fit was much better above 5meV , but worse below. Lok’s model has optical phonon scattering dominating optical absorption, with IIM scattering appearing to have a negligible effect. In his results, the lower gains at higher impurity concentrations are due to IIM scattering from the light hole to the heavy hole band, causing a loss of inversion. This has a more significant effect on the optical gain than the extra optical absorption caused by the IIM scattering. Using our algorithm that weights the choice of IIM scattering angle, we see the same.

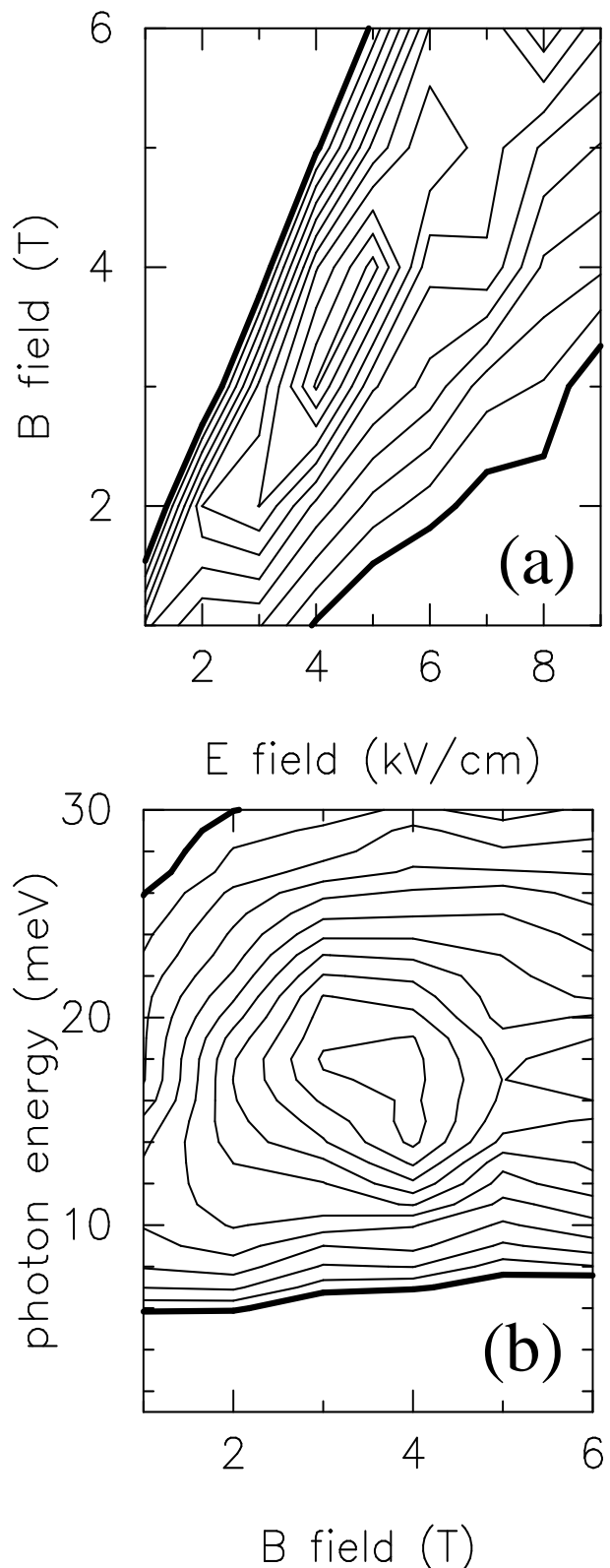


FIG. 2: Gain in p-Ge, $n_i = 0.025 \times 10^{16} \text{cm}^{-3}$, laser photon polarization in the \vec{E} direction. (a) The net gain after free-carrier optical absorption has been taken into account. The thick contour is at zero, and contours step up in gain by 0.025cm^{-1} . (b) The net gain as a function of magnetic field and photon frequency (for the optimum electric field).

IV. GALLIUM ARSENIDE

The obvious III-V material to investigate is GaAs, as it is already widely used for many other applications [9, 10, 11]. It has zone center effective masses of roughly $m_{HH} \approx 0.50$ and $m_{LH} \approx 0.07$, with a ratio rather similar to that in germanium (Ge). The main difference compared to Ge is that GaAs has additional scattering processes – it is a polar material, so there are also piezo-electric phonon (ACP) processes and polar optical phonon (OPP) processes to consider. While the piezo-electric processes are usually not very significant, the polar optical phonons have a significant role, largely because their strength is inversely dependent on the phonon momentum.

TABLE II: The relative frequencies of different scattering types in GaAs at a point of optimum gain: $E = 8\text{kV/cm}$ $[2\bar{1}\bar{1}]$, $B = 7\text{T}$ $[0\bar{1}1]$ and $n_i = 0.025 \times 10^{16}$. There were a total of 16000 scatterings, and the hole was in the LH band for $180 \pm 25\text{ps}$, and the HH band for $687 \pm 5\text{ps}$. The average time between collisions in the LH and HH bands were $t_{LH} = 3.8\text{ps}$ and $t_{HH} = 0.7\text{ps}$ respectively. NB: $m_{HH}/m_{LH} \approx 8$; $r_{stream} \approx 1.7\text{ps}^{-1}$

Transition	ACD	ACP	IIM	OPD	OPP	Total
HH \rightarrow HH	899	186	383	4198	9001	14667
HH \rightarrow LH	43	4	34	188	297	566
LH \rightarrow LH	3	7	181	1	9	201
LH \rightarrow HH	222	41	193	8	102	566

Simulations were done for a range of electric and magnetic field magnitudes, from 2kV/cm to 20kV/cm, and 2T to 12T. The maximum fields were chosen somewhat higher than is usually practicable in experiment to ensure we covered the full range of interest. For $n_i = 0.025 \times 10^{16}\text{cm}^{-3}$, the E/B ratio for optimum gain was 1.14 (cf 1.25 for Ge).

A full array of simulations was done for $n_i = 0.025 \times 10^{16}\text{cm}^{-3}$, an electric field direction of $E[2\bar{1}\bar{1}]$, and a magnetic field direction of $B[0\bar{1}1]$ (relative to the crystal axes). This moderate impurity concentration showed a best net gain of 0.08cm^{-1} at high fields ($\sim 8\text{kV/cm}$, 7T) (as shown in Fig. 3). Although reasonable inversion-gain occurs down to fields of a few kV/cm (or T), the optical absorption is strong enough to spoil it except at higher fields. The net gain for a range of different field orientations were also checked at the optimum 8kV/cm, 7T point, but $E[2\bar{1}\bar{1}]$ & $B[0\bar{1}1]$ were confirmed as giving the greatest gain. In general, the orientation dependence can be significant, with sometimes up to a factor of two difference in the net gain.

Next, simulations were done at higher and lower impurity concentrations for the best-gain value of E and B fields. The higher impurity concentration ($n_i = 0.100 \times 10^{16}\text{cm}^{-3}$) results indicated that there is at best a marginal gain. This is because the increased impurity scattering has two effects. First, the extra scattering increases the calculated optical absorption; and secondly, impurity scattering is more efficient at depopulating the LH band by producing LH \rightarrow HH scattering than it is at repopulating it with HH \rightarrow LH scatterings. A table of the

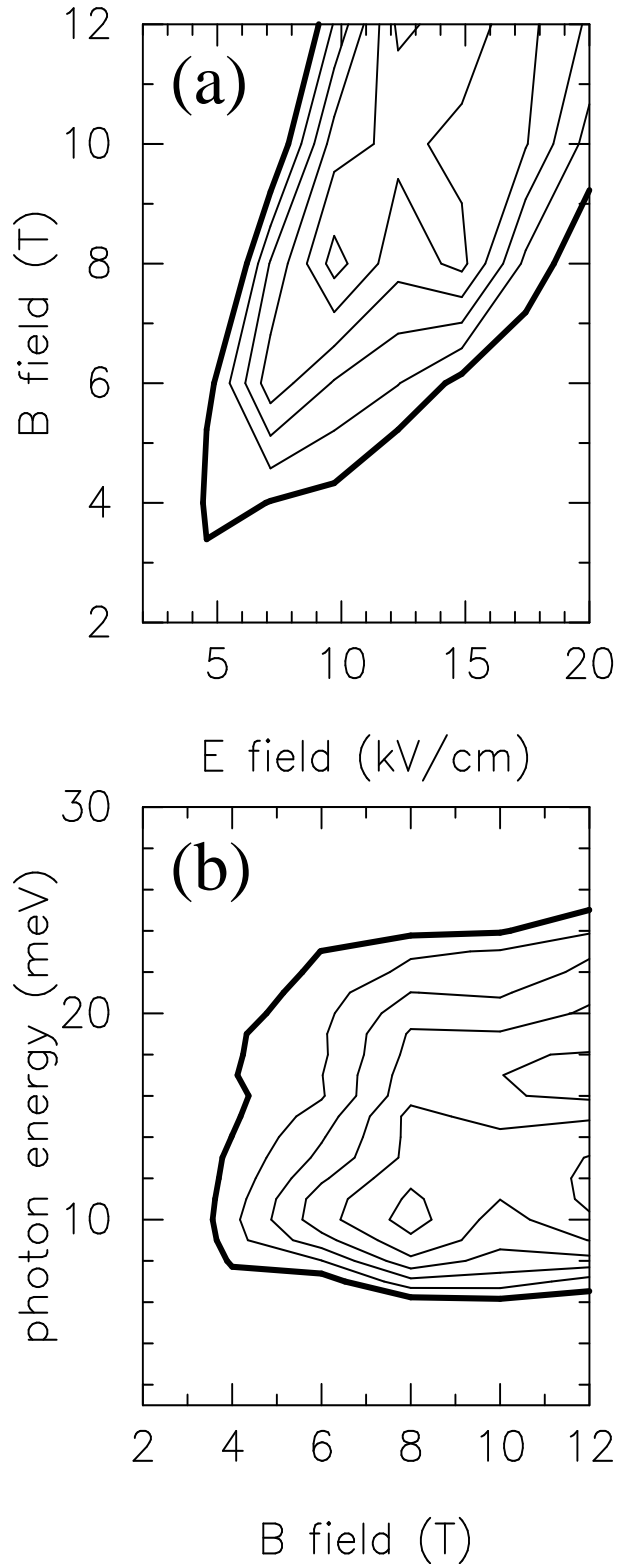


FIG. 3: Gain in p-GaAs, $n_i = 0.025 \times 10^{16}\text{cm}^{-3}$, laser photon polarization in the \vec{E} direction. (a) The net gain after free-carrier optical absorption has been taken into account. The thick contour is at zero, and contours step up in gain by 0.025cm^{-1} . (b) The net gain as a function of magnetic field and photon frequency (for the optimum electric field).

relative frequencies of the different scattering types at $E = 8$ kV/cm $[2\bar{1}\bar{1}]$, $B = 7$ T $[0\bar{1}\bar{1}]$ is given in Table II.

The lower impurity concentration simulations ($n_i = 0.005 \times 10^{16} \text{cm}^{-3}$) show a better net-gain cross-section $\sigma_I - \sigma_A$. However, since the number of holes in the simulation is related to the impurity (doping) concentration, fewer impurities also means fewer holes, and fewer holes means that the gain per length λ is proportionally reduced. So although the net-gain cross-section is up to double that for $n_i = 0.025 \times 10^{16} \text{cm}^{-3}$, the net-gain per cm reduces to $\lambda \sim 0.04 \text{cm}^{-1}$.

The dependence of the net gain on the polarization of the output light is small. Typically one orientation (of B , E , or $E \times B$) is better than the other two, which are otherwise very similar. Output light polarized in the B direction requires the hot-hole laser to be in the Voigt configuration, but E polarized output can be achieved by either the Voigt or Faraday configurations. In our simulations, the polarization in the electric field (E) direction gave the best gain; this contrasts with the comments in Ref. [13] saying that a polarization parallel to the magnetic field (B) minimises heavy hole scattering and hence the optical absorption.

V. INDIUM ANTIMONIDE

An often mentioned candidate for a III-V hot-hole laser is p-InSb, because its effective mass ratio m_{HH}/m_{LH} is much greater than that in either GaAs or Ge. The simple argument is that since the light hole cyclotron orbits can be more tightly confined in k -space, this leads to a more pronounced inversion. However, since our simulation code cannot treat light hole Landau levels, we restricted our simulations to magnetic fields under 2T; and so were unable to make predictions at the higher fields where the confined light hole cyclotron orbits might give a significantly increased gain.

TABLE III: The relative frequencies of different scattering types in InSb at a point of optimum gain: $E = 1.8 \text{kV/cm}$ $[0\bar{1}\bar{1}]$, $B = 1 \text{T}$ $[100]$ and $n_i = 0.025 \times 10^{16}$. There were a total of 16000 scatterings, and the hole was in the LH band for $55 \pm 17 \text{ps}$, and the HH band for $1326 \pm 13 \text{ps}$. The average time between collisions in the LH and HH bands were $t_{LH} = 4.5 \text{ps}$ and $t_{HH} = 1.4 \text{ps}$ respectively. NB: $m_{HH}/m_{LH} \approx 30$; $r_{stream} \approx 0.55 \text{ps}^{-1}$

Transition	ACD	ACP	IIM	OPD	OPP	Total
HH \rightarrow HH	1681	47	648	3610	9679	15665
HH \rightarrow LH	15	0	16	47	70	148
LH \rightarrow LH	2	0	37	0	0	39
LH \rightarrow HH	50	1	50	3	44	148

From Fig. 4 we can see that the peak gain at $n_i = 0.025 \times 10^{16} \text{cm}^{-3}$ is about 0.05cm^{-1} , and the trend is the usual one for better inversion at higher fields. The dependence of the net gain on the polarization of the output light is small, as for GaAs, and indeed Ge. For InSb, the best field orientation is not an electric field direction of $[2\bar{1}\bar{1}]$, and a magnetic field direction of $[0\bar{1}\bar{1}]$; but $E[0\bar{1}\bar{1}]$ $B[100]$. A table of the relative

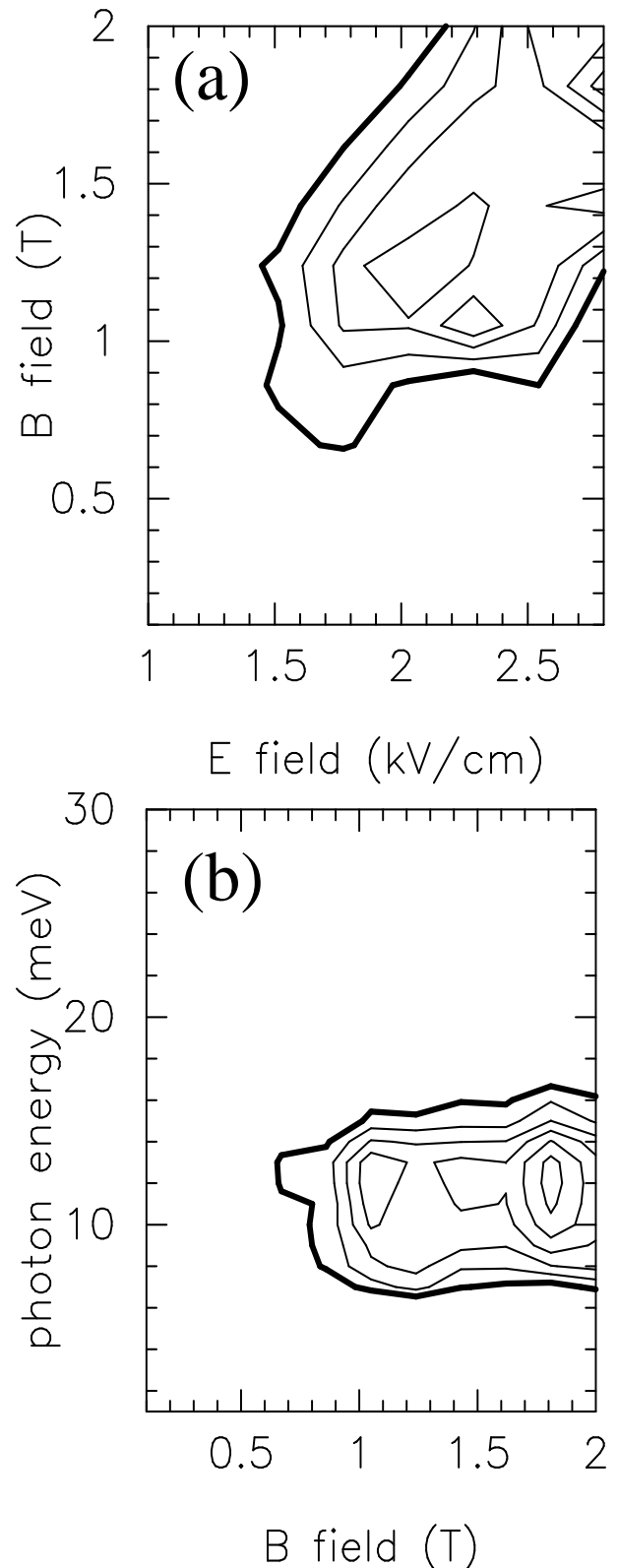


FIG. 4: Gain in p-InSb, $n_i = 0.025 \times 10^{16} \text{cm}^{-3}$, laser photon polarization in the \vec{E} direction. (a) The net gain after free-carrier optical absorption has been taken into account. The thick contour is at zero, and contours step up in gain by 0.025cm^{-1} . (b) The net gain as a function of magnetic field and photon frequency (for the optimum electric field).

frequencies of the different scattering types at $E = 1.8$ kV/cm $[0\bar{1}1]$, $B = 1.0$ T $[100]$ is given in Table III.

As with GaAs, simulations were done for InSb at the same higher and lower impurity concentrations ($n_i = 0.100, 0.005 \times 10^{16} \text{cm}^{-3}$) for the best-gain value of electric and magnetic fields. The higher impurity concentration produced a prediction of no net gain – for the same reasons as when the higher impurity concentration reduced the gain in GaAs. The low impurity concentration gave reduced gain, with the resulting smaller hole concentration again overcoming the slight increase in gain cross section.

VI. DISCUSSION

These results indicate a number of important considerations for hot-hole laser operation in bulk III-V materials. Firstly, control of the impurity concentration is critical, as e.g. in GaAs, the material can go from no net-gain through its peak back to no net-gain with only a factor of 20 or so range in impurity concentration. Secondly, as in Ge, the orientation of the electric and magnetic fields with respect to the crystallographic axes is important – while the difference in the amount of net gain from the best choice in InSb to the second best choice is not large, the region over which it can be obtained is. This then is particularly important if there are restrictions on the maximum fields allowed. Finally, it is clear that the performance in p-GaAs and p-InSb is not as good as in p-Ge hot-hole lasers; the main reason being that the non-polar p-Ge does not have the polar optical phonon (OPP) and acoustic pizeoelectric phonon (ACP) scattering processes, and that this extra scattering has a more significant negative effect than the benefits of the improved effective mass ratio.

For GaAs, OPP scattering transfers more holes into the LH band than deformation optical phonon (OPD) scattering – however, it also scatters more out. As a result, the net transfer of holes into the LH band is similar for both optical phonon processes. The much greater LH \rightarrow HH rate for OPP is due to the small momentum transfer Δk in such processes: the OPP rate is inversely proportional to Δk . Also note that the GaAs ionised impurity scattering (IIM) rates are roughly double those for Ge – this is largely due to the difference in dielectric constants, which appear to the fourth power in the denominator of the scattering rate prefactor. The dielectric constant for Ge is about 16, compared to 13 for GaAs. Also, the dielectric constant affects the screening length which also alters the IIM scattering rates. Unfortunately it is not possible to easily compare the IIM scattering rates and dielectric constants between Ge or GaAs and InSb, as their effective mass ratios are so different – $(m_{HH}/m_{LH})_{Ge,GaAs} \approx 8$, but $(m_{HH}/m_{LH})_{InSb} \approx 30$.

In InSb the net transfer of holes into the LH band is similar for both optical phonon processes. Also the HH \rightarrow LH scattering rates in InSb are consistently lower than for GaAs, which is due largely to the lower LH density of states caused by InSb's lower LH effective mass.

Note that for both GaAs and InSb in the above discussion, a large effective mass ratio m_{HH}/m_{LH} was either not mentioned

as important (GaAs), or was regarded as bad (InSb). This is in contrast to simple arguments which state that large ratio is good because it helps ensure efficient streaming up the HH band whilst retaining good cyclotron orbits in the LH band – unfortunately, too large a ratio brings the LH density of states down too low, inhibiting population transfer to the LH band and hence inhibiting inversion. The simple arguments also miss the influential role of the dielectric constant in controlling impurity scattering rates (GaAs).

Next, we need to consider the criteria given in past analyses as described in section I. Here we can clarify their roles using the simple rate-equation model (Eqs. 1–3) described earlier. For $N_L \ll N_H + N_{H+}$, the fraction of population in the LH band in the steady state is

$$P = \frac{N_L}{N_H + N_{H+}} = \frac{\gamma r_{OP} r_{stream}}{r_{LH} (r_{OP} + r_{stream} + r_{HH})}. \quad (4)$$

The three important criteria are: (i) a large γ , which means a small m_{HH}/m_{LH} ratio (but not so small as to disrupt either the HH streaming or LH cyclotron orbits); (ii) that r_{HH} should be as small as possible compared to $r_{stream} + r_{OP}$; and (iii) that r_{LH} should be much less than the smaller of r_{stream} or r_{OP} . We have extracted these scattering rates from our optimum gain Monte Carlo simulations, and using these in eqn.(4) gives the same trends as is observed for the net gain – $P = 0.10, 0.08, 0.05$ for the Ge, GaAs, and InSb simulations respectively. Also, the simulation γ 's were generally close to the ratio of effective masses.

In summary, we have presented a rate equation model of hot-hole lasers and simulation results that clarify the roles of performance criteria presented in earlier analyses. We show that in general III-V materials should have an acceptable performance, which contrasts with previous criteria that suggested more optimistically that (e.g.) InSb should make an excellent hot-hole laser. This demonstrates the need to treat the lasing cycle as a whole, as in our rate equation model, rather than treating each step in isolation. Finally, the performance of III-V hot-hole lasers might most easily be improved by moving to a modulation doped quantum wells – thus eliminating the impurity scattering by moving the impurities away from the active region, and giving us opportunity to engineer the band structure.

Acknowledgements

We would like to thank C.A.M. Haarman for implementing polar phonon scattering in the simulation code. This work is funded by the European Commission via the program for Training and Mobility of Researchers.

- [1] Opt. Quantum Electron. Vol. **23**, Special Issue Far-infrared Semiconductor Lasers, (Eds. E. Gornik and A.A. Andronov, Chapman and Hall, London 1991).
- [2] J. N. Hovenier, A. V. Muravjov, S. G. Pavlov, V. N. Shastin, R. C. Strijbos, and W. Th. Wenckebach, Appl. Phys. Lett. **71**, 443-445 (1997).
- [3] R.C. Strijbos et al., in Hot Carriers in Semiconductors, edited by K. Hess, J.-P. Leburton, and U. Ravaioli (Plenum Press, New York, 1996), pp. 631-633.
- [4] F. Keilmann and R. Till, Semicond. Sci. Technol. **7**, B633 (1992).
- [5] E. Brundermann et al., Infrared Phys. Technol. **36**, 59 (1995).
- [6] R.C. Strijbos, J.G.S. Lok and W.Th. Wenckebach, J. Phys. Condens. Matter **6**, 7461 (1994).
- [7] J.N. Hovenier, T.O. Klaassen, W. Th. Wenckebach and A.V. Muravjov, S.G. Pavlov and V.N. Shastin, Appl. Phys. Lett. **72**, 1140 (1998).
- [8] A.V. Murajov, S.H. Withers, R.C. Strijbos, S.G. Pavlov, V.N. Shastin, R.E. Peale, Appl. Phys. Lett. **75**, 2882 (1999).
- [9] *Physics of quantum electron devices*, ed. F. Capasso, (Springer-Verlag, Berlin, 1990).
- [10] M. Shur, *GaAs devices and circuits*, (Kluwer, 1987).
- [11] F. Capasso, C.Gmahl, D.L. Sivco, A.Y.Cho, *Quantum cascade lasers*, Physics World **12**, no. 6, 27 (1999).
- [12] The time take to get from the bottom of the heavy hole band to ϵ_{LO} is $t_{stream} = (\sqrt{m^* \epsilon_{LO}}/E) \times 1.07$ (ps) where m^* is relative to the electron mass, ϵ_{LO} is in meV, and E is the electric field in kV/cm; $r_{stream} = 1/t_{stream}$. If it does not scatter, it will return to low energy by completing a cyclotron orbit in a time $T_{cH} = m_{HH}/eB$.
- [13] V.N. Shastin, Opt. Quantum Electron. **23**, S111 (1991).
- [14] S. Komiyama, S. Kuroda, I. Hosaka, Y. Akaska, N. Iizuka, Opt. Quantum Electron. **23**, S133 (1991).
- [15] A.A. Andronov, Infrared and Millimeter Waves **16**, Chapter 5, 149 (1986).
- [16] J.G.S. Lok, unpublished.
- [17] C. Moglestu, *Monte Carlo simulation of semiconductor devices*, (Chapman & Hall, London, 1993).
- [18] E.O. Kane, in *Semiconductors and Semimetals*, eds. R.K. Willardson and A.C. Beer, (Academic Press, New York, 1966), Vol. **1**, page 75.
- [19] B.K. Ridley *Quantum Processes in Semiconductors*, (Clarendon Press, Oxford, 1988).
- [20] L. Reggiani, in *Hot electron transport in semiconductors*, ed. L. Reggiani, (Springer-Verlag, Berlin, 1985), page 7.
- [21] *Submillimeter lasers by hot holes in semiconductors*, Ed. A.A. Andronov, (AN-USSR IPF, Gorky, 1986).
- [22] Absorption was compared for for $E = 2\text{kV/cm}$ $[1\bar{1}0]$, $B = 1.3\text{T}$ $[\bar{1}\bar{1}1]$, temperature 10K, $n_i = 1.3 \times 10^{14}\text{cm}^{-1}$.